The dependence of traction evolution on the earthquake source time function adopted in kinematic rupture models

Alessio Piatanesi, Elisa Tinti and Massimo Cocco

Istituto Nazionale di Geofisica e Vulcanologia, Department of Seismology and Tectonophysics, Rome, Italy

Eiichi Fukuyama

National Research Institute for Earth Science and Disaster Prevention,Tsukuba, Japan

Abstract. We compute the temporal evolution of traction by solving the elasto-dynamic equation and by using the slip velocity history as a boundary condition on the fault plane. We use different source time functions to derive a suite of kinematic source models to image the spatial distribution of dynamic and breakdown stress drop, strength excess and critical slip weakening distance (D_c). Our results show that the source time functions, adopted in kinematic source models, affect the inferred dynamic parameters. The critical slip weakening distance, characterizing the constitutive relation, ranges between 30% and 80% of the total slip. The ratio between D_c and total slip depends on the adopted source time functions and, in these applications, is nearly constant over the fault. We propose that source time functions compatible with earthquake dynamics should be used to infer the traction time history.

1. Introduction

The space and time history of shear stress produced on the fault plane during an earthquake rupture has been explored by several recent studies (*Bouchon et al*., 1998; *Dalguer et al*., 2002; *Zhang et al*., 2003; *Day et al*., 1998). The dynamic traction evolution is commonly inferred from kinematic rupture models with the ambition to constrain the fault constitutive behavior (*Ide and Takeo,* 1997; *Guatteri and Spudich*, 2000). Ground motion time histories are inverted to image a kinematic rupture model. The corresponding temporal evolution of slip on the fault plane is obtained either by assuming an analytical expression for the source time function (single window inversion) or by assuming that each fault point can slip more than once (multi-window inversion). The latter provides the slip time history as part of the solution, although the temporal resolution of the retrieved kinematic model is rather low, while the former imposes a priori the source time function. Because the temporal evolution of dynamic traction on the fault plane is retrieved by the slip time history, the choice of the source time function might affect the inferred dynamic parameters. This is the main motivation of the present study.

Most of these investigations solve the elasto-dynamic equation to compute the dynamic traction at selected points on the fault plane, where the kinematic model is supposedly well resolved. The traction evolution allows the calculation of dynamic stress drop and strength excess on the assumed fault plane (*Mikumo and Miyatake*, 1995; *Bouchon*, 1997) as well as the estimate of the critical slip weakening distance (D_c). For instance, *Ide and Takeo* (1997) evaluated values of D_c ranging between 50 and 100 cm for the 1995 Kobe earthquake. Several other recent studies have inferred in similar ways values of the slip weakening distance ranging between 20% and 90% of the total final slip (*Pulido and Irikura*, 2000; *Guatteri et al*., 2001; *Peyrat et al*., 2001). Moreover, an unexplained correlation between the total slip and the inferred D_c values has been

obtained by some investigators (*Zhang et al.*, 2003). In the present study we aim to understand if the source time functions adopted in kinematic models can bias the retrieved dynamic parameters and partially explain the variability of D_c estimates. *Guatteri and Spudich* (2000) also emphasized the limitations in estimating the critical slip weakening distance by modeling ground motion waveforms. In particular, they concluded that both the adoption of spatial and temporal smoothing constraints in the formulation of the inverse problem and the modeling of low-frequency seismic waves can bias the inferred values of D_c. Here we face the same problem from a different point of view.

The values of the critical slip weakening distance computed from kinematic inversions and ground motion modeling are two order of magnitude larger than those inferred in laboratory experiments (*Okubo and Dieterich*, 1984; *Ohnaka and Yamashita*, 1989) or used in numerical simulations performed with laboratory-derived constitutive laws (*Cocco and Bizzarri*, 2002, and *Bizzarri and Cocco*, 2003). This means that there is still an open debate within the scientific community on the actual size of the critical slip weakening distance. In this study we aim to contribute to this debate by estimating the dependence of traction evolution on the source time function chosen to model ground motion waveforms.

2. Method

We use a 3-D finite difference dynamic code to calculate the stress time history on the earthquake fault plane (*Andrews*, 1999). The stress is computed through the fundamental elasto-dynamic equation (*Ide and Takeo*, 1997). The total dynamic traction in each fault position is calculated by the sum of two contributions: the instantaneous term depending on slip velocity and the dynamic load related to the previous slip history. In the present study we impose the slip velocity as a boundary condition. In other words, each node belonging to the fault plane is forced to move with a prescribed slip velocity time history. In this way we do not need to specify any constitutive relation and the dynamic traction evolution is a result of the calculations.

The space and time distribution of slip velocity (V) is derived from an input kinematic rupture model. We use different slip velocity distributions, defined as

$$V(\boldsymbol{\xi},t) = \dot{f}(t - t_r(\boldsymbol{\xi})) \cdot d(\boldsymbol{\xi}), \qquad (1)$$

by adopting different source time functions $\dot{f}(t)$ (whose unit is s^{-1}) for a given distribution of final slip $d(\boldsymbol{\xi})$. In (1) $\boldsymbol{\xi}=(\xi_1,\xi_2)$ represents the local coordinates on the fault plane, t is time and $t_r(\boldsymbol{\xi})$ the rupture time. This means that the shape of the slip velocity function all over the fault is chosen *a priori*, while the rupture time and the slip amplitude can vary depending on the node position. For our simulations, we assume a homogeneous half-space discretized with $\Delta x=\Delta y=\Delta z=100$ m grid cell size, $\Delta t=0.01$ s and an initial shear stress $\tau_0=20$ MPa; the density is $\rho = 2700$ kg/m^3 and the body wave velocities are $V_P = 5.2$ km/s and $V_S = 3.0$ km/s.

2.1. Adopted source time functions

In order to investigate the resulting dynamic traction evolution, we use three distinct source time functions $\dot{f}(t)$ characterizing slip velocity, which have the following analytical forms:

$$f_1 = \dot{f}(t) = H(t)\frac{2}{T_R}\left[1 - \tanh^2\left(\frac{2}{T_R}\left(2t - \frac{3}{2}T_R\right)\right)\right] \qquad (2a)$$

$$f_2 = \dot{f}(t) = H(t)\frac{2}{T_R}e^{\frac{-2t}{T_R}} \quad (2b)$$

$$f_{3,4} = \dot{f}(t) = H(T_R - t)\frac{2}{\pi T_R}\left(\frac{-t+T_R}{t}\right)^{1/2} \quad (2c)$$

In these equations $H(t)$ is the Heaveside function, T_R is the rise time and the others quantities are defined above. These relations define source time functions already known in the literature: (2a) and (2b) are similar to those used by *Cotton and Campillo* (1995) in their kinematic inversion method, while (2c) has been proposed by *Nielsen and Madariaga* (2003). The latter have demonstrated that function (2c) is obtained either in steady-state or self-similar model solutions and that it is compatible with a constant frictional level inside the slipping area. We emphasize that only the function (2c) is based on elasto-dynamic considerations. To avoid the singularity or discontinuity of some analytical relations, the numerical representation of $\dot{f}(t)$ is obtained by smoothing the functions in time: we convolve $\dot{f}(t)$ with a moving triangular window of assigned width. In particular, for function (2c) we use two smoothing windows with different durations of 0.07 s and 0.37 s; the corresponding functions are named in the following f_3 and f_4, respectively. All the functions are normalized to have a unit integral over time. The slip velocity time histories defined above are shown in Figure 1 (red lines). The function f_1 is characterized by a very smooth rupture onset; on the contrary, f_3 is characterized by an abrupt onset and a larger peak value. Function f_2 has been truncated to impose the prescribed duration, function f_1 tends to zero exponentially, while function $f_{3,4}$ has an analytical expression with zero slip velocity at T_R. To simplify the analysis we have chosen the same rise time for all the time functions (T_R=1 s).

3. Simulations with a uniform slip model

We perform our numerical simulations by assuming a rupture model similar to that proposed for the 2000 Western Tottori (Japan) earthquake (M_w=6.8) consisting of a vertical fault plane with a left lateral strike-slip motion (*Fukuyama et al*., 2003). The fault is 26 km long and 14.4 km wide. We first consider a uniform slip model (d = 1 m) characterized by a constant rupture velocity (2.0 km/s). We therefore derive four kinematic models, which differ only in the adopted source time functions. We have also compared the synthetic ground velocities calculated at several receivers by using these different kinematic models as input for the isochrones approach (*Spudich and Xu*, 2002). We found that in the frequency band 0.1 - 2.0 Hz the simulated time histories are almost identical, while they differ in the high frequency band (1.5 - 15 Hz). In particular, the seismograms computed with f_3 have higher frequency content and larger peak velocities (roughly twice than the others). This simple test confirms that these rupture models are “kinematically” equivalent in the frequency band usually adopted in waveform inversions (0.05-1.5 Hz).

The four adopted source models are the input parameters in our dynamic algorithm. Figure 1 shows the time history of slip, slip velocity and the resulting dynamic traction (left panels) as well as the traction as a function of slip (right panels) calculated for a particular target point. Our numerical results illustrate that the traction evolution within the cohesive zone exhibits the slip weakening behavior, although the shape of the slip weakening curve strongly depends on the assumed source time function. The total dynamic traction shows an evident restrengthening for all source models (healing of slip, see Figure 1). Our results

show that the yield stress and the frictional stress amplitudes depend on the adopted source time function, because the slip velocity peaks are different (see Figure 1). We emphasize the difficulty in using source time functions that are particularly sharp. In fact, even with a spatial discretization of 100 m in the numerical algorithm, the traction evolution inferred by using the time function f_3 of figure 1 shows evidence of numerical dispersion (see the shaded area in figure 1), which is due to a spatial under-sampling of slip velocity. Therefore, the required spatial and temporal resolution of the dynamic model depends on the shape of the selected source time function. It is interesting to note that the traction computed with the function f_4 is in good agreement with the analytical form, well known in the literature (*Nielsen and Madariaga*, 2003 and references therein). The numerical simulations shown in Figure 1 demonstrate that the inferred values of D_c strongly depend on the assumed source time function: the smoothest function (f_1) gives an estimate of D_c exceeding 80% of total slip, while the sharpest one (f_3) yields D_c of the order of 30% of the final slip. These results are consistent with the conclusions of previous investigations, that pointed out the high sensitivity of D_c estimates to fault parameterization (*Day et al.*, 1998; *Guatteri and Spudich*, 2000).

4. Simulations with a heterogeneous slip model

We now examine the dynamic traction evolution calculated from a heterogeneous kinematic model. We use the slip distribution proposed by *Iwata and Sekiguchi* (2001) for the 2000 Western Tottori earthquake. For the purpose of our study, we oversimplified this model by retaining only the rupture times and the strike component of the slip distribution (shown in Figure 2). We consider two source time functions among those shown in Figure 1, namely f_1 and f_4, using a constant rise time of 1 s. The resulting two different slip velocity models are used as input for the dynamic code to compute the spatio-temporal evolution of total traction: the inferred spatial distribution of dynamic stress drop and strength excess are shown in Figure 3. This figure shows that high values of strength excess are found in correspondence of zones where the crack tip decelerates. The adopted source time function affects the amplitudes of both strength excess and dynamic stress drop: the source time function f_4 produce larger strength excess amplitudes than those calculated from f_1, while the contrary happens for the stress drop values. This is due to the fact that f_4 has a steeper initial slope (see Figure 1) and generates larger slip accelerations than f_1.

We show in Figure 4 the distribution of the breakdown stress drop (defined by *Ohnaka and Yamashita*, 1989, as the difference between the yield and the frictional stress) and the critical slip weakening distance calculated for f_1 and f_4. This figure illustrates that the breakdown stress drop is less dependent on the adopted source time function than strength excess or dynamic stress drop. This result suggests that the two source time functions affect the amplitudes of both yield and frictional stresses of nearly the same amount. Moreover, the spatial distribution of D_c inferred for both f_1 and f_4 is correlated with the final slip distribution. This observation is consistent with the dynamic modeling results obtained by *Zhang et al*. (2003). The ratio between D_c and the final slip strongly depends on the adopted source time functions.

5. Discussion and conclusive remarks

We have shown that the choice of the source time function in kinematic rupture models affects the calculation of dynamic parameters in numerical algorithms which use the slip history

as a boundary condition on the fault plane. The most interesting results of this study concern the inferred value and the spatial distribution of the critical slip weakening distance (D_c). We find that different source time functions yield different D_c values ranging between 30% and 80% of the total slip. Our simulations show an evident correlation between the spatial distribution of D_c and the final slip over the fault plane, in agreement with previous studies. Moreover, the ratio between D_c and final slip value is nearly constant and controlled by the adopted source time function. We also point out that the same source time function, smoothed in different way, yields different D_c values. This occurs because the smoothing operation modifies the initial slope and the associated slip acceleration. Further investigations are needed to interpret the retrieved correlation between D_c and final slip values. Our simulations point out that different dynamic stress drop patterns can be associated with the same slip distribution. This might represent an important limitation to constrain the slip weakening distance using kinematic models derived from ground motion modeling.

In this synthetic test study, we have chosen a spatio-temporal resolution that is better than that used in kinematic modeling of ground motion waveforms recorded during real earthquakes. Therefore, we conclude that the retrieved pattern of strength excess and dynamic stress drop, as well as the critical slip weakening distance, are biased by the limited temporal resolution and the low frequency representation of the adopted source time functions. The methodology used in this study to infer the traction evolution and the slip weakening curves is common to many recent investigations. However, in these numerical approaches the source time function is chosen a priori, and it might not be consistent with the dynamic propagation of an earthquake rupture. We have verified this inadequacy when we have modeled heterogeneous distribution of rupture times. In fact, in those fault portions where the rupture accelerates or decelerates, the peak, the shape and the duration of slip velocity do not change as expected by rupture dynamics, because they are imposed a priori. This condition limits the capability to reconstruct the time history of dynamic traction overall the fault plane. The possibility that kinematic models might not be dynamically consistent should be taken into account to constrain stress or strength during earthquake ruptures. In this study we have presented some tests and further investigations are needed to propose solutions. However, we suggest that it should be recommended to use source time functions which are compatible with earthquake dynamics.

Acknowledgments. We would like to thank Paul Spudich, Stefan Nielsen and Andrea Bizzarri for the helpful discussions and criticism. We also wish to thank Haruko Sekiguchi for providing us her rupture model of the Tottori earthquake. We benefit of the comments of M. Bouchon, S. Day and two anonymous referees who helped us to improve the text.

References

Andrews, D.J., Test of two methods for faulting in finite-difference calculations, *Bull. Seismol. Soc. Am.,* 89, 4, 931-937, 1999.

Bizzarri, A. and Cocco M., Slip weakening behaviour during the propagation of dynamic ruptures obeying rate and state dependent friction laws, *J. Geophys. Res.,* 108(B8), 2373, doi: 10.1029/2002JB002198, 2003.

Bouchon, M., The state of stress on some faults of the San Andreas system as inferred from near-field strong motion data, *J. Geophys. Res,*102, B6, 11731-1744, 1997.

Bouchon, M., Campillo M and Cotton F., Stress field associated with the rupture of the 1992 Landers, California, earthquake and its implications concerning the fault strength at the onset of the earthquake, *J. Geophys. Res.,* 103, B9, 21091-21097, 1998.

Cocco, M, and Bizzarri A., On the slip-weakening behaviour of rate-and state dependent constitutive laws, *Geophys. Res. Lett.,* 29,11, doi:10.1029/2001GL013999, 2002.

Cotton, F. and Campillo M., Frequency domain inversion of strong motions : application to the 1992 Landers earthquake, *J. Geophys. Res.,* 100, 3961-3975, 1995.

Dalguer, L.A., Irikura K., Zhang W., Riera J.D., Distribution of dynamic and static stress changes during 2000 Tottori (Japan) earthquake: brief interpretation of the earthquake sequences; foreshocks, mainshock and aftershocks, *Geophys. Res. Lett.,* 29, 16, doi:10.1029/2001GL014333, 2002.

Day, S.M., Yu G. and Wald D.J., Dynamic stress changes during earthquake rupture, *Bull. Seismol. Soc. Am.,* 88(2), 512-522, 1998.

Fukuyama, E., Ellsworth W.L, Waldhauser F. and Kubo A., Detailed fault structure of the 2000 Western Tottori, Japan, earthquake sequence, *Bull. Seismol Soc. Am.,* in press, 2003.

Guatteri, M. and Spudich P., What can strong-motion data tell us about slip-weakening fault-friction laws?, *Bull. Seismol. Soc. Am.*, 90 (1), 98-116, 2000.

Guatteri, M., Spudich P. And Beroza G., Inferring rate and state friction parameters from a rupture model of the 1995 Hygo-ken Nanbu (Kobe) Japan earthquake, *J. Geophys. Res.,* 106, B11, 26511-26521, 2001.

Ide, S. and Takeo M., Determination of constitutive relations of fault slip based on seismic wave analysis, *J. Geophys. Res.,* 102, B12, 27379-27391, 1997.

Iwata, T. and Sekiguchi H., Inferences of earthquake rupture process from strong-motion records, presented at the Symposium from Strong-Motion Network, 2001.

Mikumo, T. and Miyatake T., Heterogeneous distribution of dynamic stress drop and relative fault strength recovered from the results of wave-form inversion – the 1984 Morgan-Hill, California earthquake, *Bull. Seismol. Soc. Am.,* 85 (1), 178-193, 1995.

Nielsen, S. and R. Madariaga. On the self-healing fracture mode, *Bull. Seismol. Soc. Am.,* 93(6), 2375-2388, 2003.

Ohnaka, M. and Yamashita T., A cohesive zone model for dynamic shear faulting based on experimentally inferred constitutive relation and strong motion source parameters, *J. Geophys. Res.,* 94, 4089-4104, 1989.

Okubo, P.G. and Dieterich J.H., Effect of physical fault properties on friction instabilities produced on simaulated faults, *J. Geophys. Res.,* 89, 5817-5827, 1984.

Peyrat, S., Olsen K and Madariaga R., Dynamic modeling of the Landers earthquake, *J. Geophys. Res.,* 106, B11, 26467-26482, 2001.

Pulido, N and Irikura K., Estimation of dynamic rupture parameters from the radiated seismic energy and apparent stress, *Geophys. Res. Lett.,* 27, 23, 3945-3948, 2000.

Spudich, P. and Xu L., Software for calculating earthquake ground motions from finite faults in vertically varying media, CD accompanying International Handbook of Earthq. and Eng, Seismol., V.2, 2002.

Zhang, W. Iwata T., Irikura K., Sekiguchi H. and Bouchon M., Heterogeneous distribution of the dynamic source parameters of the 1999 Chi-Chi, Taiwan, earthquake, *J. Geophys. Res.*, 108, B5, 2232, doi:10.1029/2002JB001889, 2003

A. Piatanesi, E. Tinti and M. Cocco, Istituto Nazionale di Geofisica e Vulcanologia, Via di Vigna Murata 605, 00143 Rome, Italy. (e-mail: piatanesi@ingv.it, tinti@ingv.it, cocco@ingv.it)

E. Fukuyama, National Research Institute for Earth Science and Disaster Prevention, Tsukuba, Japan. (e-mail: fuku@bosai.go.jp)

(Received …; revised …; accepted ….)

PIATANESI ET AL.: THE DEPENDENCE OF TRACTION EVOLUTION

PIATANESI ET AL.: THE DEPENDENCE OF TRACTION EVOLUTION

Figure 1. Normalized time histories of slip, slip velocity and total dynamic traction (left panels) calculated with the source time functions defined in equations (2a-b-c). Right panels show the resulting slip weakening behaviors in dimensional units. The arrows depict the estimated value of the critical slip weakening distance. Numbers indicate the absolute amplitude values in each panel.

Figure 2. Slip and rupture time distribution on the fault plane for the 2000 Western Tottori earthquake used in this study.

Figure 3. Strength excess and dynamic stress drop distribution calculated on the fault plane, using the source time functions f1 and f4 shown in figure 1. The rupture time distribution is superimposed to each panel.

Figure 4. Distribution of breakdown stress drop and critical slip weakening distance on the fault plane retrieved for the two source time functions f1 and f4. The rupture time distribution is superimposed to each panel.

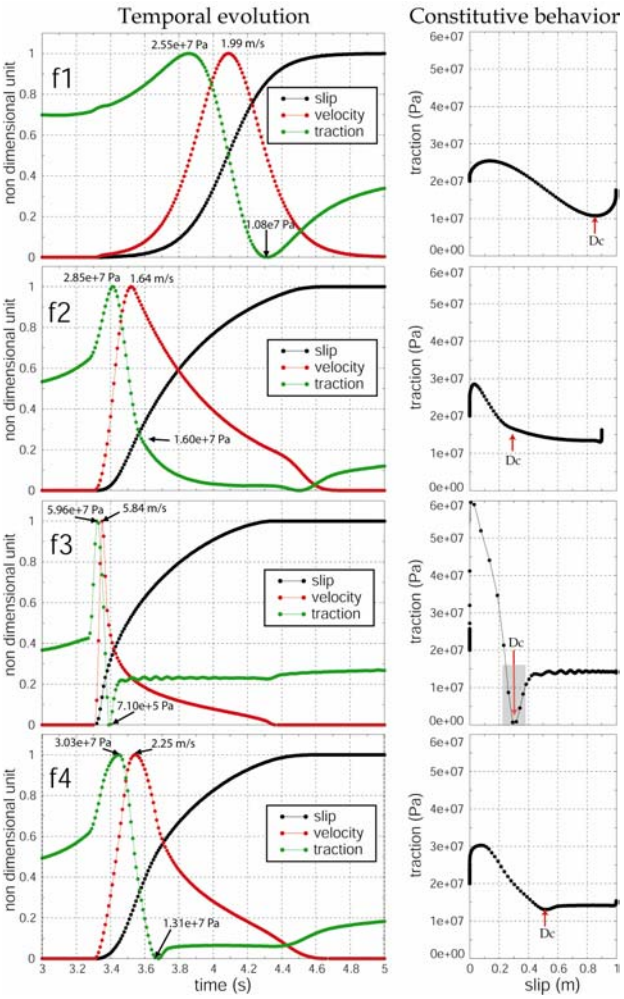
Temporal evolution
Constitutive behavior
f1
f2
f3
f4
slip
velocity
traction
non dimensional unit
traction (Pa)
time (s)
slip (m)
Dc
2.55e+7 Pa
1.99 m/s
1.08e7 Pa
2.85e+7 Pa
1.64 m/s
1.60e+7 Pa
5.96e+7 Pa
5.84 m/s
7.10e+5 Pa
3.03e+7 Pa
2.25 m/s
1.31e+7 Pa

Figure 1

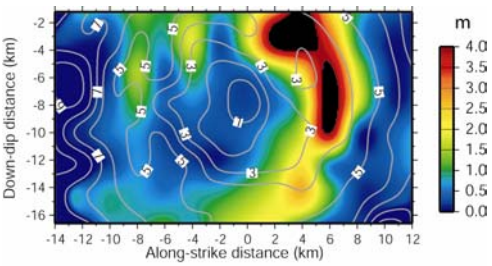
m
4.0
3.5
3.0
2.5
2.0
1.5
1.0
0.5
0.0
Down-dip distance (km)
-2
-4
-6
-8
-10
-12
-14
-16
Along-strike distance (km)
-14 -12 -10 -8 -6 -4 -2 0 2 4 6 8 10 12

Figure 2

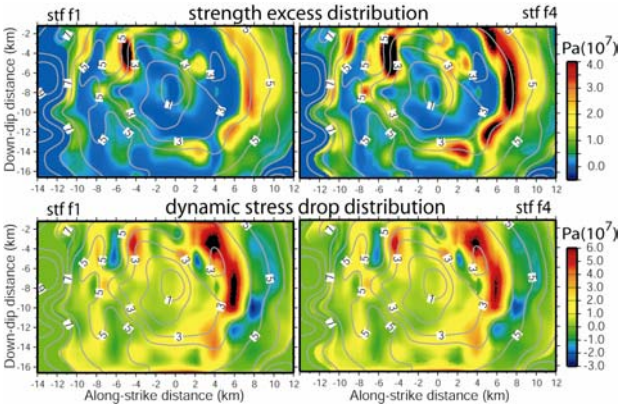
stf f1
strength excess distribution
stf f4
Pa(10^7)
4.0
3.0
2.0
1.0
0.0
Down-dip distance (km)
stf f1
dynamic stress drop distribution
stf f4
Pa(10^7)
6.0
5.0
4.0
3.0
2.0
1.0
0.0
-1.0
-2.0
-3.0
Down-dip distance (km)
Along-strike distance (km)
Along-strike distance (km)

Figure 3

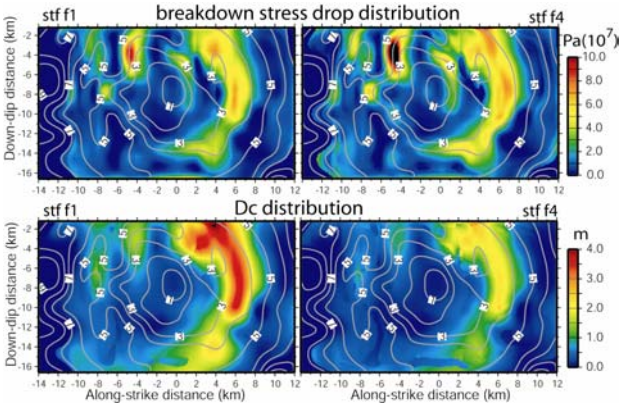
stf f1
breakdown stress drop distribution
stf f4
Pa(10^7)
10.0
8.0
6.0
4.0
2.0
0.0
Down-dip distance (km)
stf f1
Dc distribution
stf f4
m
4.0
3.0
2.0
1.0
0.0
Down-dip distance (km)
Along-strike distance (km)
Along-strike distance (km)

Figure 4